catalysts

MDPI

Article

Highly Active Carbon Material Derived from *Carica papaya* Fruit Juice: Access to Efficient Photocatalytic Degradation of Methylene Blue in Aqueous Solution under the Illumination of Ultraviolet Light

Muhammad Ali Bhatti [1], Elmuez Dawi [2], Aneela Tahira [3], Khalida Faryal Almani [1], Shymaa S. Medany [4], Ayman Nafady [5], Zulifqar Ali Solangi [6], Umair Aftab [7] and Zaffar Hussain Ibhupoto [8,*]

[1] Centre for Environmental Sciences, University of Sindh Jamshoro, Jamshoro 76080, Pakistan; mali.bhatti@usindh.edu.pk (M.A.B.); khalida.almani@usindh.edu.pk (K.F.A.)
[2] Nonlinear Dynamics Research Centre (NDRC), Ajman University, Ajman P.O. Box 346, United Arab Emirates; e.dawi@ajman.ac.ae
[3] Institute of Chemistry, Shah Abdul Latif University, Khairpur Mirs 66020, Pakistan; aneela.tahira@salu.edu.pk
[4] Department of Chemistry, Faculty of Science, Cairo University, Cairo 12613, Egypt; shymaasamir80@yahoo.com
[5] Department of Chemistry, College of Science, King Saud University, Riyadh 11451, Saudi Arabia; anafady@ksu.edu.sa
[6] Department of Chemical Engineering, Mehran University of Engineering and Technology, Jamshoro 76080, Pakistan; zulifqar.solangi@muet.edu.pk
[7] Department of Metallurgy and Materials, Mehran University of Engineering and Technology, Jamshoro 76080, Pakistan; umair.aftab@faculty.muet.edu.pk
[8] Dr. M. A. Kazi Institute of Chemistry, University of Sindh, Jamshoro 76080, Pakistan
* Correspondence: zaffar.ibhupoto@usindh.edu.pk

Citation: Bhatti, M.A.; Dawi, E.; Tahira, A.; Almani, K.F.; Medany, S.S.; Nafady, A.; Solangi, Z.A.; Aftab, U.; Ibhupoto, Z.H. Highly Active Carbon Material Derived from *Carica papaya* Fruit Juice: Access to Efficient Photocatalytic Degradation of Methylene Blue in Aqueous Solution under the Illumination of Ultraviolet Light. *Catalysts* **2023**, *13*, 886. https://doi.org/10.3390/catal13050886

Academic Editor: Da-Ren Hang

Received: 17 April 2023
Revised: 10 May 2023
Accepted: 12 May 2023
Published: 14 May 2023

Abstract: Herein, we describe a cost-effective, efficient, sustainable, and environmentally friendly pyrolytic method for the synthesis of highly active carbon materials from *Carica papaya* fruit juice for the photodegradation of various pollutants, such as methylene blue (MB), in aqueous solutions using ultraviolet (UV) light. Various analytical techniques were used to examine the morphology, crystal quality, functional group chemistry, particle size distribution, and optical properties of the materials. For evaluating the performance of the newly prepared carbon material, various photocatalyst parameters were investigated, including initial dye concentration, catalyst dose, pH of dye solution, cyclic stability, and scavenger studies. The obtained findings attest that the optimal degradation efficiency of carbon material for high MB concentrations (2.3×10^{-5} M) is around 98.08%, whereas at low concentrations of MB (1.5×10^{-5} M) it reaches 99.67%. Degradation kinetics indicate that MB degrades in a first-order manner. Importantly, as the pH of the dye solution was adjusted to ~11, the degradation rate increased significantly. The scavenger study indicated that hydroxyl radicals were the predominant species involved in the degradation of MB. In addition, active surface site exposure and charge transfer were strongly associated with efficient MB degradation. On the basis of its performance, this newly developed carbon material may prove to be an excellent alternative and promising photocatalyst for wastewater treatment. Furthermore, the synthetic approach used to produce carbon material from *Carica papaya* fruit juice may prove useful for the development of a new generation of photoactive materials for environmentally friendly applications, as well as for the production of hydrogen from solar energy.

Keywords: *Carica papaya* fruit juice; carbon material; methylene blue

1. Introduction

The textile industry releases a large amount of effluent, including dyes and other chemicals, that can have an adverse impact on both humans and ecosystems when mixed with

rivers or other bodies of water. Globally, textile effluent treatment and other environmental contamination have become serious concerns in recent years. The use of biomass [1] as a major source of carbon material is currently promoted as a solution to this problem. In recent years, carbon materials have been considered as a potential candidate for photocatalysis and adsorption applications, owing to their specific surface area, large porosity, and high activity. However, the drawback of these material is identified in view of the low availability of standardized processes along with the limited information about their specific applications. For instance, functionalized graphite materials having diverse and typical functional groups, or doped graphitic materials with certain dangling bonds, are associated with the adsorption of several ionic and molecular substances. This type of adsorption on the functionalized graphite surface is suggested to be chemisorption, whereas the adsorption performed by the weak Vander Waal forces via π-π interactions between the aromatic molecules and the graphitic material is simply physical adsorption [2]. Graphene oxide is a typical carbon-based material that favors attraction and hence the removal of cationic dye because of the presence of oxygenated groups in graphene oxide; however, pristine graphene may be able to adsorb both cationic and anionic dyes through π-π interactions [2]. The photocatalytic performance accompanied by the semiconducting material with rich defect chemistry and surface-oxygenated or nitrogen-doped groups fills the gap of sp2 on the carbon material [3]. The diversity of sp^2 in carbon materials enables surface modifications for use in several applications. These surface modifications have shown a highly efficient role in driving both processes of adsorption and photocatalysis. The surface modification is carried out by producing composite systems such as metal/carbon composites [4–8] and metal oxide/carbon composites for the photocatalytic reactions of both anionic and cationic dyes [9,10].

Recent studies have demonstrated that green carbon precursors can be synthesized from milk, fruits, vegetables, hair, caramel, honey limeade, grapefruit peel, linseed, xylan, bombyx mori silk, and xylitol [11–17]. In general, it has been shown that plant extracts containing a variety of bioactive molecules, including tannins, polyphenols, flavonoids, citric acid, tartaric acid, and ascorbic acid, are capable of producing nanoparticles if they contain acids (tannin, polyphenols, and flavonoids), bases (alkaloids), and neutral compounds (carbohydrates) [18]. However, the synthesis of carbon materials from biomass or its waste with enhanced photocatalytic applications is rarely investigated. Hence, it is highly desirable to develop a facile, low-cost, eco-friendly and scalable method for the synthesis of carbon materials with promising performance for photocatalytic applications.

We propose, in this work, a facile hydrothermal carbonization approach for the synthesis of a highly active carbon material from *Carica papaya* juice. Several chemical compounds in *papaya* have antioxidant properties, including caffeic acid, myricetin, quercetin, alpha-tocopherol, papain, benzyl isothiocyanate (BiTC), kaempferol, and flavonoids. Compounds like these are important phytochemicals, with functional groups, such as carboxyl, hydroxyl, and amine, that make them ideal for the treatment of water and wastewater. Researchers have also suggested that flavonoids contained in plant biomass may serve as scavengers for photocatalysis [19–21]. As part of our ongoing research endeavors, we emphasized, in this study, the significance of carbon materials in enhancing the photocatalytic degradation of the carcinogenic methylene blue (MB) dye in aqueous media and via illumination with UV light.

2. Result and Discussion

2.1. Crystalline Arrays, Morphology, and Optical Characterization of As-Prepared Carbon Material from Carica papaya Fruit Juice

An SEM examination of the typical surface morphology of carbon material prepared from *Carica papaya* juice is shown in Figure 1a,b. As can be seen from the SEM images, the carbon has a sheet-like shape and carries small particles on its surface, as is typical of carbon. In Figure 1b, a homogeneous sheet-oriented shape with similar properties to graphite is shown. The FTIR spectrum of the presented carbon material is presented in Figure 1c, which

provides information about the chemistry of the functional group. The results indicate that the band gap of 3447 cm^{-1} is a result of (O-H) hydroxyl groups bound to the surface of the carbon material, while the band gap of 2926 cm^{-1} corresponds to the frequency of C-H stretching vibrations. An apparent band associated with the stretching band wavenumber of the S-H group was observed at 2512 cm^{-1}, and the typical features of the C=O carbonyl bond were observed at 1792 cm^{-1}. The FTIR band at 1631 cm^{-1} is associated with stretching vibrations around C-O and bending vibrations of N-H groups [22], whereas the band at 1431 cm^{-1} is attributed to the chemical environments of C-N, N-H, and –COO. The FTIR analysis of carbon surfaces indicates that recurring groups such as -NH_2, -OH, and -COO are bound to the surface, and this observation has been substantiated by published studies [23–26]. The as-prepared carbon was tested optically in an aqueous solution, and the obtained UV-visible spectrum is shown in Figure 1d. The figure illustrates an inset of a shoulder peak consisting of three distinct absorbance regions at 351, 356, and 361 nm. It has been suggested that the absorbance band at 351 nm is a consequence of the n–π* transition of the CO band structure [27–29]. These optical results clearly indicate that the carbon material derived from the *Carica papaya* juice exhibited similar characteristics to those carbon-dot-like materials previously reported elsewhere [30,31].

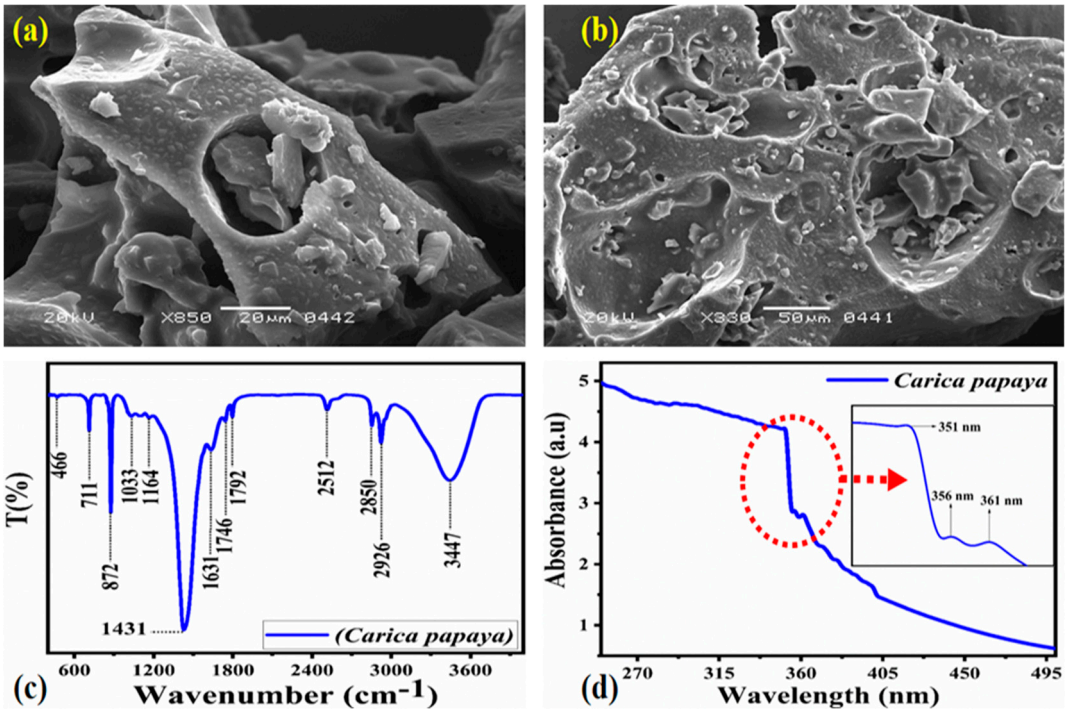

Figure 1. (**a**,**b**) SEM images of low and high magnification of carbon material, (**c**) FTIR spectrum and (**d**) absorbance spectrum and the inset wavelength of synthesized carbon material from Carica papaya juice.

As shown in Figure 2a, a powder XRD was also used to determine the crystalline nature of the synthesized carbon material. Diffraction patterns could not be clearly resolved, and weak reflections were observed for 001, 002, and 101 at 19°, 28°, and 44°, respectively. According to XRD analysis, the carbon material exhibits crystalline features closely related to graphite; however, the weak reflection suggestes that the material is most likely contained in an amorphous phase. Based on the XRD patterns, the results are reasonably consistent with those found in previous studies on graphite-based carbon material [32]. A camera image of the carbon material illuminated with UV light for three minutes is shown in Figure 2a. This image displays the luminescent characteristics of carbon as it is prepared. Figure 2b shows the results of a dynamic light scattering (DLS) experiment used to determine the carbon material's particle size distribution. The particle size distribution of the

carbon material under DLS was determined using Zetasizer Nano (ZS). It was determined that the average particle size distribution was approximately 1148 nm in diameter. As shown in Figure 2b, the DLS spectrum consists of two distribution peaks, and each peak represents the relative quantity of particle size distribution.

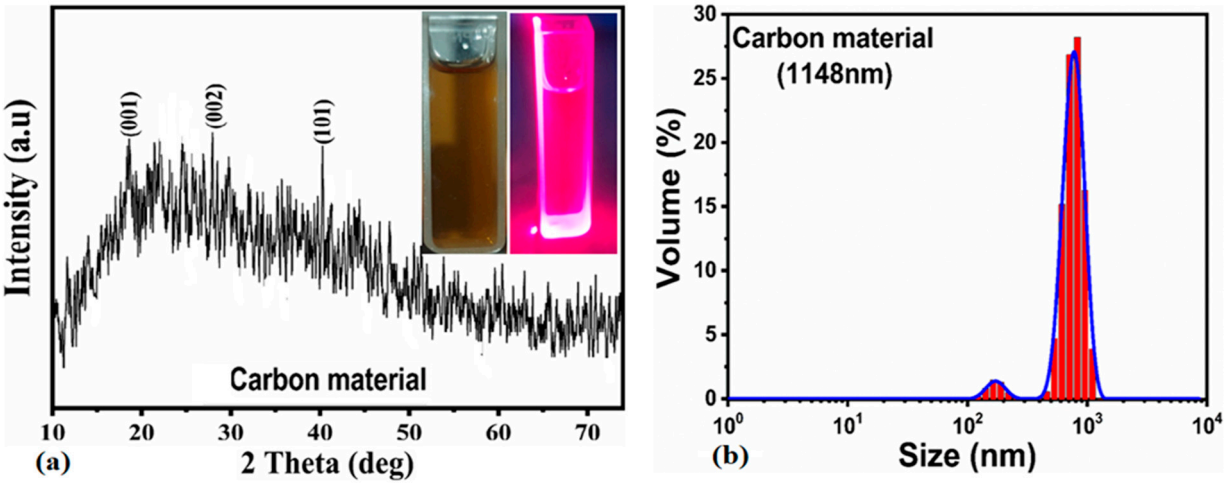

Figure 2. (**a**) XRD pattern and inset display luminescence images of carbon material in daylight and UV light and (**b**) histogram showing the size distribution of synthesized carbon material.

2.2. Photocatalytic Application of As-Prepared Carbon Material against the Photodegradation of Methylene Blue

The carbon material prepared from *Carica papaya* juice was also used as a low-cost, simple, and eco-friendly catalyst to treat wastewater. Prior to the evaluation of the catalytic performance of the prepared carbon material, a 2.3×10^{-5} M concentration of MB solution was irradiated with UV light without carbon material as shown in Figure 3. Figure 3a, in particular, illustrates the decrease in the absorbance of the MB solution upon irradiation with UV light for certain time intervals. However, the decrease in absorbance is very slow and insignificant, thereby suggesting a kinetically slow degradation of MB when irradiated with UV light only. According to the results of the kinetic study, Figure 3b,c illustrates the kinetics of the reaction in the absence of the catalyst. Based on the observations, it appears that the UV light irradiation of the MB solution has a negligible impact on reaction speed as well as a limited influence on reaction kinetics. The degradation efficiency of the 2.3×10^{-5} M MB solution was also examined. According to Figure 3d, the degradation efficiency of MB was around 3%, which is a very low value. Therefore, UV light has a limited role in degrading MB, and thus the development of new photocatalysts with improved functions is highly demanded.

2.2.1. Initial Dye MB Concentration and Photocatalyst Dose Study

We have evaluated the photocatalytic performance of carbon materials prepared from *Carica papaya* juice, as well as their initial MB dye concentration, catalyst doses of five, ten, and fifteen milligrams, dye solution pH, recycling stability, and the identification of active radicals responsible for MB photodegradation in aqueous solutions. This study used MB concentrations of 2.3×10^{-5} M and 1.5×10^{-5} M. In Figure 4, different catalyst doses are illustrated, such as 5 mg for X, 10 mg for Y, and 15 mg for Z. To begin with, dye concentrations were tethered to specific catalyst doses in the dark. The adsorption and desorption equilibria were established by exposing them to UV light. As a result of the presence of carbon material under mechanical stirring, an adsorption rate of 2–3% could be expected. According to our findings, the carbon material was primarily involved in the photocatalytic oxidation of MB in the presence of UV light, while the adsorption process was very limited. Every 25 min, the absorbance variation was recorded for 2.3×10^{-5} M as displayed in Figure 4a–c and 1.5×10^{-5} M as shown in Figure 4d–f. The absorbance of each

dye concentration decreased as the sweeping time of the UV light was increased. According to Figure 4a,d, a carbon catalyst containing 5 mg greatly enhanced dye degradation. The degradation rate, on the other hand, increased significantly in response to an increase in catalyst dose from 10 mg to 15 mg, as shown in Figure 4b,c,e,f. The results of this analysis indicate that the carbon material from the *Carica papaya* juice was actively exposed during the UV light irradiation of the MB solution, which generated enough radicals to effectively oxidize the MB under UV light illumination. It is noteworthy that the carbon material performs relatively better when the dye concentration is low. Therefore, the UV photons had the greatest ability to reach the surface of the catalyst, and they activated the surface and accelerated the oxidation reaction rate of the MB, as shown in Figure 4d–f. In spite of this, there is the possibility that the surface of the carbon material can be covered with dye molecules when there is a high concentration of MB present. This reduces the dye degradation effectiveness, as indicated in Figure 4a–c. Additionally, it has been demonstrated that the high concentration of MB could not support the generation of large numbers of electron–hole pairs, which could potentially produce a significant number of oxidizing radicals. Consequently, carbon materials are less efficient at high MB concentrations.

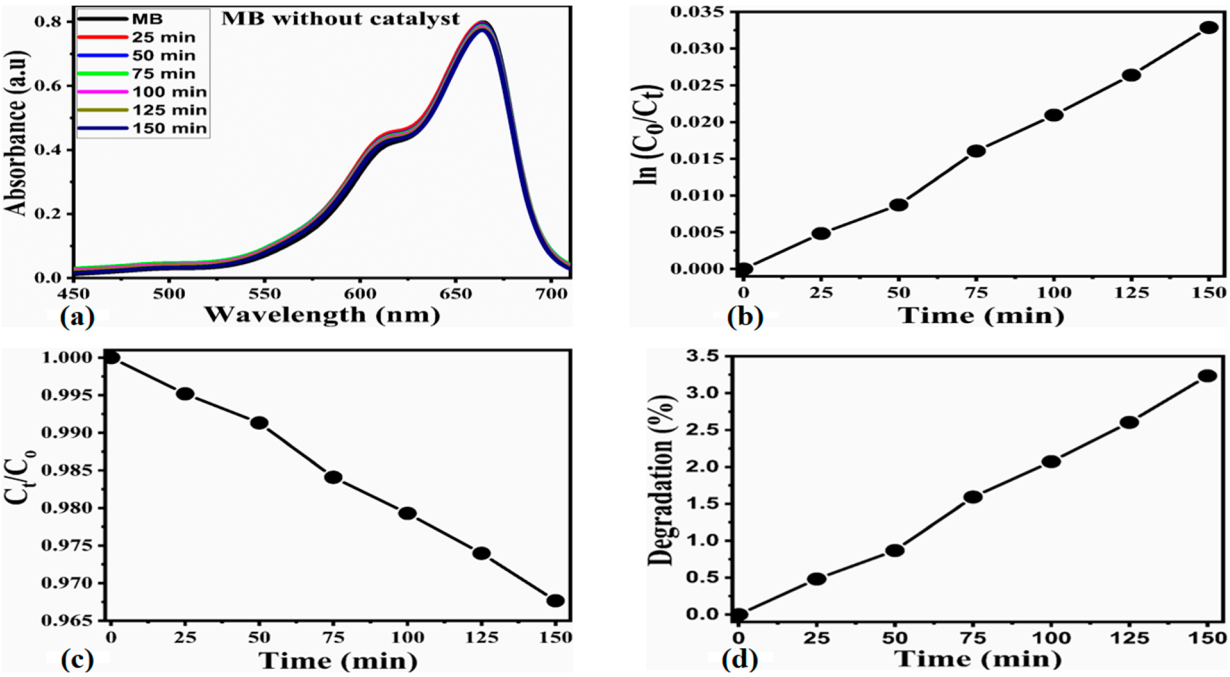

Figure 3. (**a**) UV absorbance spectra measured at concentration of 2.3 × 10^{-5} M MB dye solution without prepared photocatalyst for the time period of 150 min under ultraviolet light illumination, (**b**,**c**) kinetic reaction of MB dye degradation in the absence of photocatalyst, and (**d**) degradation (%) efficiency only with the ultraviolet light.

The kinetic study was carried out for the photodegradation of MB at both concentrations of 2.3 × 10^{-5} M and 1.5 × 10^{-5} M at 5 mg, 10 mg, and 15 mg catalyst doses of the prepared carbon material under the influence of UV light as shown in Figure 5.

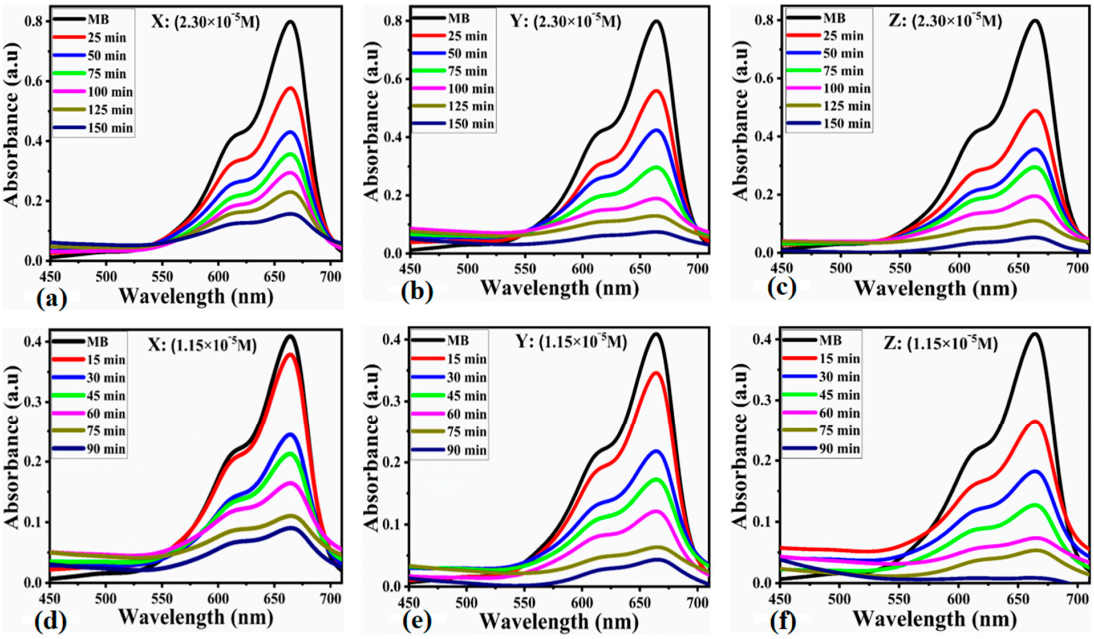

Figure 4. (**a**–**c**) UV-visible UV absorbance spectra measured at a concentration of 2.3 × 10^{-5} M MB dye solution consuming a catalyst dose of (**a**) 5 mg, (**b**) 10 mg, and (**c**) 15 mg for the time period of 150 min under ultraviolet light illumination. (**d**–**f**) UV-visible UV absorbance spectra measured at a concentration of 1.15 × 10^{-5} M MB dye solution consuming a catalyst dose of (**a**) 5 mg, (**b**) 10 mg, and (**c**) 15 mg for the time period of 90 min under ultraviolet light illumination.

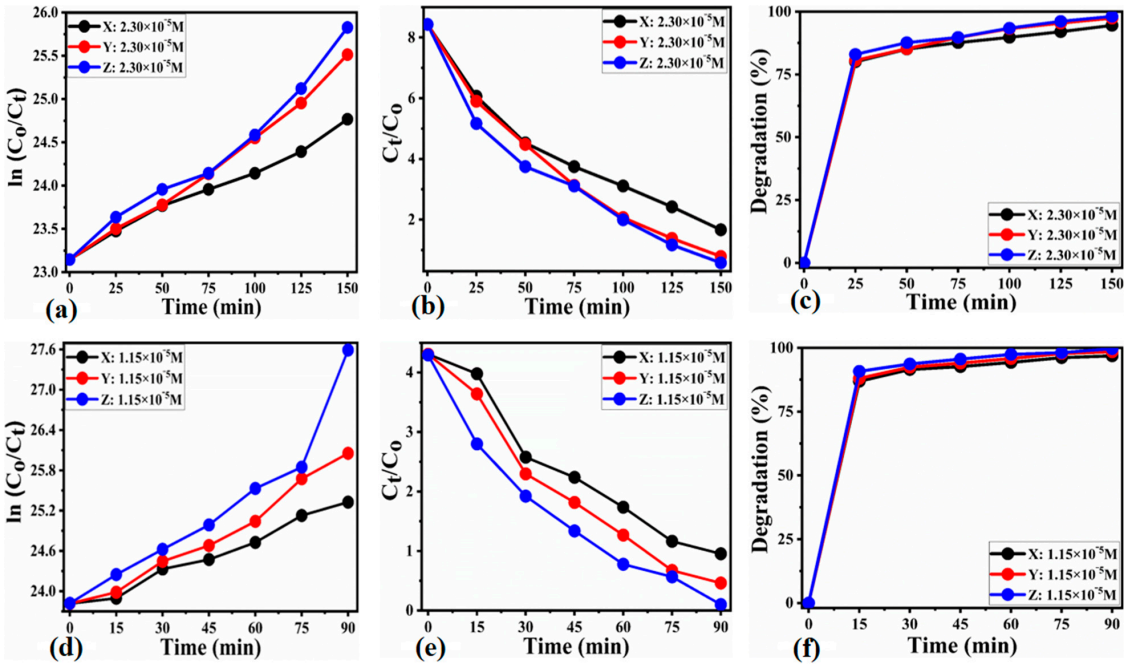

Figure 5. (**a**,**b**) Degradation kinetics of MB dye solution consuming different catalyst doses of 5 mg, 10 mg, and 15 mg at a concentration of 2.3 × 10^{-5} M MB under ultraviolet light illumination, (**c**) degradation (%) efficiency of MB concentration 2.3 × 10^{-5} M with different catalyst doses of 5 mg, 10 mg, and 15 mg for the time period of 150 min, (**d**,**e**) degradation kinetics of MB dye solution consuming different catalyst doses of 5 mg, 10 mg, and 15 mg at a concentration of 1.5 × 10^{-5} M MB under ultraviolet light illumination, (**f**) degradation (%) efficiency of MB concentration 1.5 × 10^{-5} M with different catalyst doses of 5 mg, 10 mg, and 15 mg for the time period of 90 min.

The kinetics of MB dye degradation was verified by first order through the relationships $\ln(C_t/C_0) = kt$ $\ln(C_t/C_0) = kt$. The notations C_t and C_0 are assigned to the MB concentration at certain time intervals and the initial dye concentration, respectively, whereas K is the rate constant. As shown in Table 1, the calculated rate constant values confirm that the degradation kinetics is highly favorable at low concentrations of MB relative to high concentrations of MB. The K values given in Table 1 were calculated through the measured slope to form the linear fitting of Ln (C_o/C_t) against time. A comparison of the degradation performance of the presented carbon material with that of recently published works revealed that the newly prepared carbon material is highly efficient in degrading MB in the presence of UV light [33]. It was found that the degradation efficiency of the carbon material was about 98.09% at the high concentration, as shown in Figure 5e, and about 99.6% at the low concentration, as shown in Figure 5f, using a catalyst dose of 15 mg. Compared to many published studies, these degradation efficiency values are relatively higher and confirm the use of carbon as an alternative material for the real-world treatment of wastewater [34–36]. The low concentration of dye, 1.15×10^{-5} M, has a high K value, confirming that the dye almost degraded into mineralized products such as CO_2 and H_2O. This is the dye concentration where we can say that the carbon material is highly effective in removing the MB from aqueous solution via the oxidation of MB under the illumination of UV light. For the higher concentration, 2.30×10^{-5} M, the K value is acceptable, but the dye removal is not complete and hence the optimum level of dye removal was found to be at 1.15×10^{-5} M. Furthermore, we can say that is not required to go beyond the 1.15×10^{-5} M dye concentration, because at this concentration the dye is approximately 100% degraded into harmless products.

Table 1. Summary of obtained results with carbon material from *Carica papaya*.

Sample Dose	Dye Con:	Constant (K)	Dye Con:	Constant (K)
5 mg	2.30×10^{-5} M	1.01×10^{-2} min^{-1}	1.15×10^{-5} M	1.78×10^{-2} min^{-1}
10 mg		1.50×10^{-2} min^{-1}		2.54×10^{-2} min^{-1}
15 mg		1.66×10^{-2} min^{-1}		3.67×10^{-2} min^{-1}
pH study				
pH-5	2.30×10^{-5} M	1.89×10^{-2} min^{-1}		
pH-7		2.53×10^{-2} min^{-1}		
pH-9		2.80×10^{-2} min^{-1}		
pH-11		3.19×10^{-2} min^{-1}		

2.2.2. Effect of pH of Dye Solution on the Photocatalytic Performance of Carbon Material

Additionally, it has been shown that pH has a significant effect on dye degradation rate and degradation efficiency [37]. As a result, we adjusted the pH of the MB dye solution to 2.3×10^{-5} M containing 15 mg of catalyst in the range of 5, 7, 9, and 11 by adding 0.4 M HCl and NaOH aqueous solutions under ultraviolet illumination. Figure 6a–d show the corresponding decrease in absorbance UV-visible spectra.

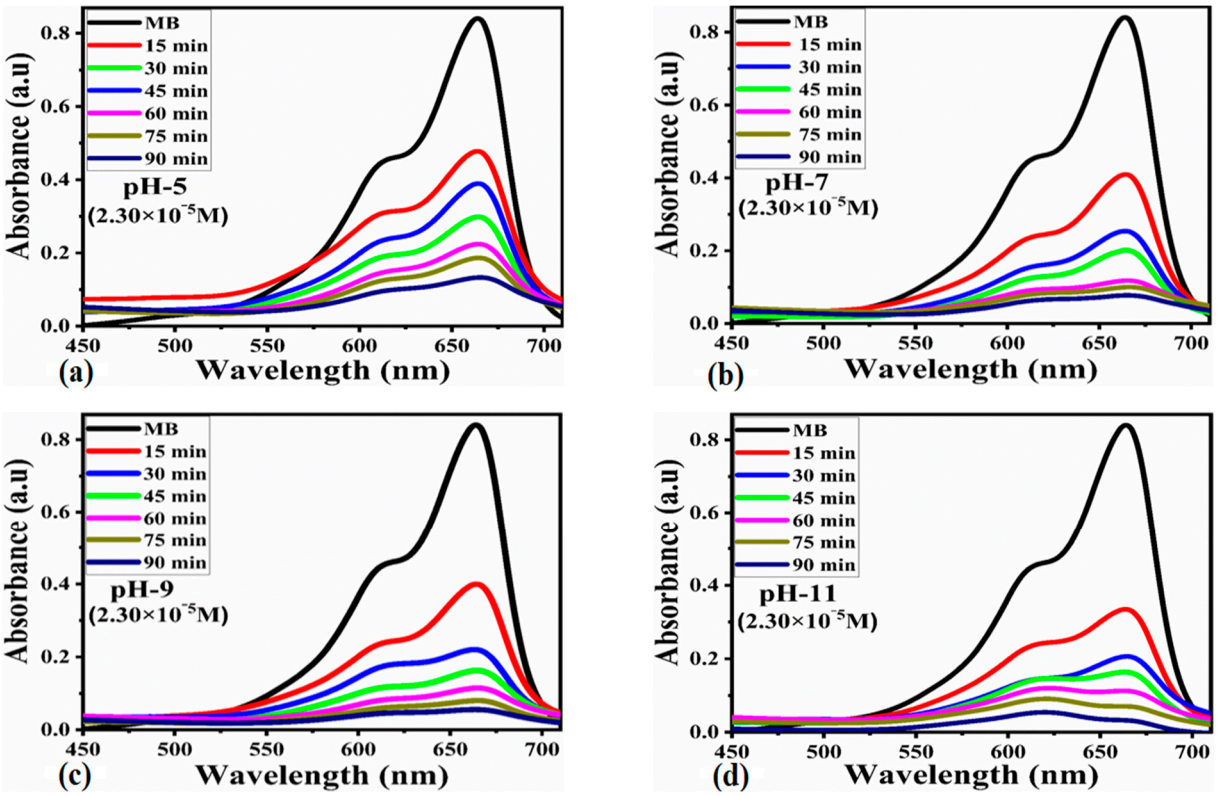

Figure 6. UV-visible UV absorbance spectra measured at a concentration of 2.30 × 10^{-5} M MB dye solution consuming a catalyst dose of only 15 mg at different pH values of the dye solution: (**a**) pH-5, (**b**) pH-7, (**c**) pH-9, and (**d**) pH-11 for the time period of 90 min under ultraviolet light illumination.

It is evident from Figure 7c that pH has provided an excellent platform for MB to degrade efficiently, and the importance of pH is particularly evident when MB solution is adjusted to pH 11. The degradation rate of MB was greatly increased when pH was used, and the dye appeared to be 100% after 90 min when pH was not adjusted at the same dye concentration as 150 min with pH adjustment. Further, it has been observed that after the degradation process, pH values have increased slightly from 5, 7, 9, and 11 to 5, 52, 7.46, 9.62, and 11.34, respectively. Approximately 98.8% of the MB was degraded efficiently at pH 11. Hydroxyl radicals may have played a significant role in the efficient degradation of MB. Studies have shown that MB becomes deprotonated in a high basic solution [38]. The generation of hydroxyl radicals is facilitated by the interaction of hydroxide ions with negative holes produced during the irradiation of photons, which in turn convert hydroxide ions into hydroxide radicals [39]. Therefore, the hydroxide radicals supported the degradation of MB when the MB solution was irradiated with carbon material [40]. Furthermore, it is well established that the nature of the photocatalyst plays an important role in determining how pH influences dye degradation; however, in the present study, the performance of the material is relatively limited in slightly acidic pH due to a low density of hydroxide ions, which results in few hydroxide radicals, thus reducing its degradation performance. We have also studied the degradation kinetics of MB under the environment of different pH values of MB in 2.3 × 10^{-5} M. Table 1 presents the degradation kinetic data collected at pH values of 5, 7, 9, and 11. Degradation kinetics in acidic pH were limited by an agglomeration of carbon material, thereby reducing surface exposure, resulting in a low degradation rate due to less interaction between the material and MB. In alkaline conditions, however, high levels of hydroxyl radicals (HO^- HO^-) were produced, which significantly impaired the degradation of MB. Additionally, due to the presence of hydroxide ions, the carbon surface is enriched with negative changes, which facilitates the adsorption of cationic MB dyes onto the carbon surface, resulting in the effective removal

of MB as shown in Figure 7d. In order to obtain a better understanding of the degradation mechanism, a scavenger study was conducted to identify the nature of radicals involved in the degradation process. The MB dye 2.3 × 10^{-5} M was irradiated with UV light in the presence of different scavenger agents, such as ascorbic acid, sodium borohydride, and ethylenediamine tetraacetate (EDTA). Generally, it has been shown that different radicals, such as hydroxyl radicals (˙OH), photogenerated holes (h^+), and superoxide radical ions ($^{\cdot}O_2^-$), have been the potential specie to degrade the dyes. Additionally, it has been demonstrated that these used scavengers are sources for the generation of hydroxyl radicals (OH) and oxygen radicals (O_2) [41] and that major degradation occurs within these radicals [42,43]. As a result of the use of EDTA as a scavenger, the degradation kinetics of MB were significantly decreased, confirming that the hydroxyl radicals are the main radicals that accelerate the degradation kinetics of MB [21,33]. This has already been demonstrated in the pH study under pH 11 under the basic conditions.

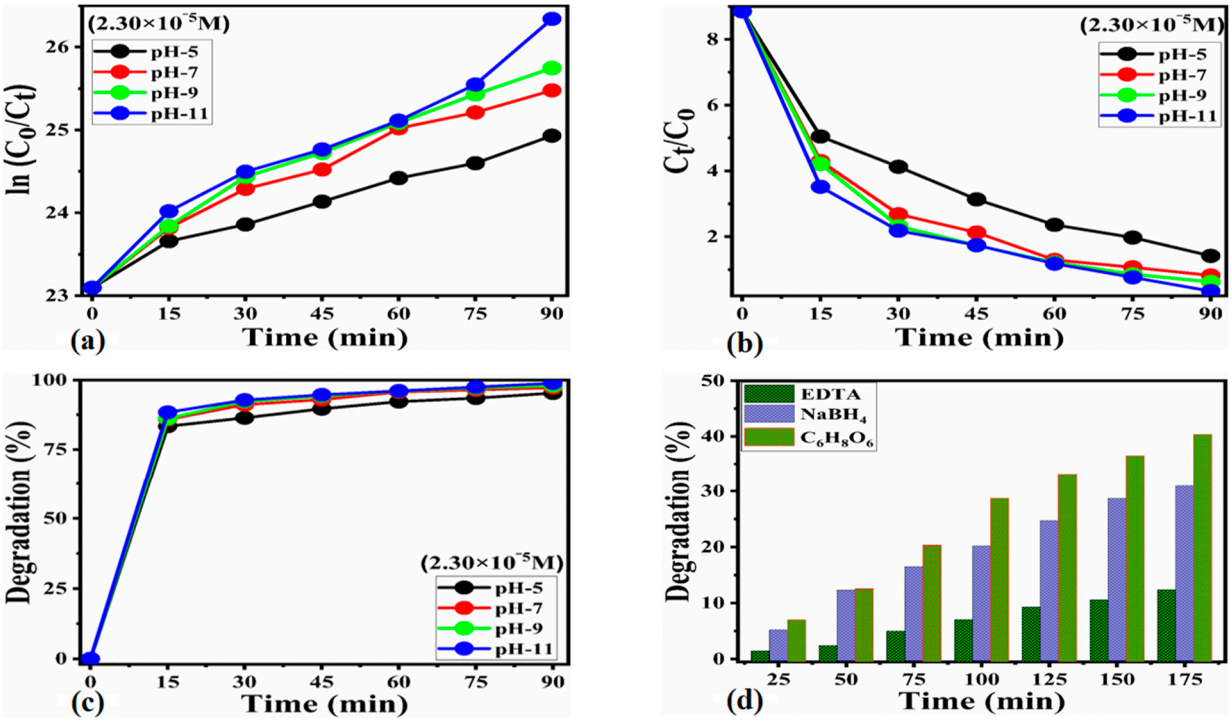

Figure 7. (**a**,**b**) Degradation kinetics of MB dye solution at a concentration of 2.30 × 10^{-5} M MB dye solution consuming a catalyst dose of only 15 mg at different pH values of the dye solution pH-5, pH-7, pH-9, and pH-11 for the time period of 90 min under ultraviolet light illumination, (**c**) degradation (%) efficiency of MB concentration 2.30 × 10^{-5} M with a catalyst dose of 15 mg for the time period of 90 min, and (**d**) degradation (%) efficiency of MB under the different scavengers at a concentration of 2.30 × 10^{-5} M MB dye solution consuming a catalyst dose of 15 mg under ultraviolet light.

We have also studied the stability and repeatability of the as-prepared carbon material using three reusability cycles and one as an initial cycle at the concentration of MB of 1.5 × 10^{-5} M as enclosed in Figure 8a. Figure 8a shows that the degradation efficiency of the carbon material towards MB degradation did not significantly change after four repeatable cycles. For four cycles, the relative degradation efficiencies were 99.67, 97.52, 95.28, and 95.18%. These cyclic stability results are highly encouraging. They provide the potential for developing a material that is low-cost, green, easy to prepare, and can be synthesized on a large scale. In addition, the amount of active site exposures was calculated through cyclic voltammetry under the non-Faradic region in 1.5 × 10^{-5} M at various scan rates as illustrated in Figure 8b. According to published work [44], electrochemical

active surface area (ECSA) calculations were carried out. The linear plot of the anode and cathode current densities against scan rates along with the estimated slope of the linear fit associated with the ECSA are shown in Figure 8c. The ESCA strongly supports the performance of carbon materials in their prepared state against MB degradation when exposed to UV radiation. Charge transfer information was also obtained using electrochemical impedance spectroscopy (EIS), as illustrated in Figure 8d. The EIS was performed at an MB concentration 1.5×10^{-5} M and the fitted data are shown in Figure 8d. The inset illustrates the equivalent circuit obtained during fitting raw EIS data. The circuit elements include solution resistance (Rs), charge transfer resistance (RCt), and constant phase element (CPE). In agreement with the reported work [44], the charge transfer resistance for the carbon material as prepared was 35.28 K ohms. As evidenced by the charge transfer results, the as-prepared carbon material performs well against MB degradation when exposed to ultraviolet light in aqueous solution under UV irradiation.

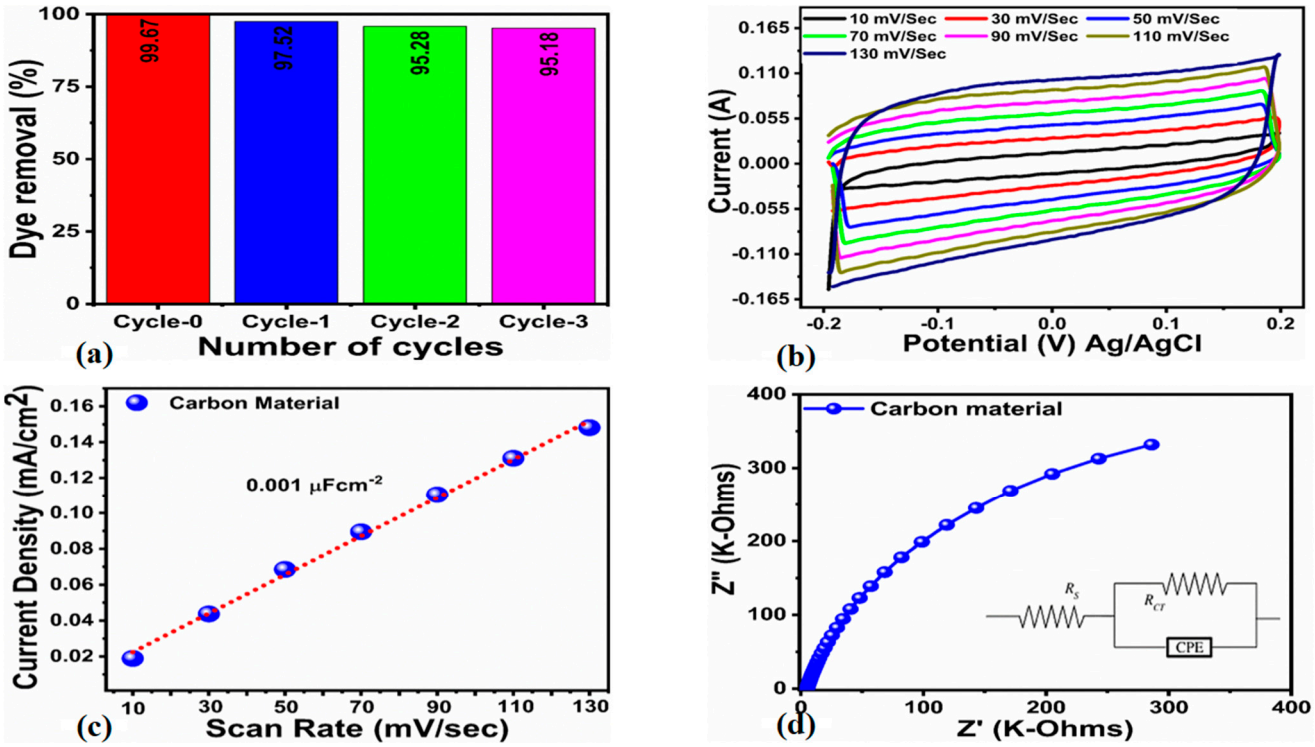

Figure 8. (**a**) Reusability test of three cycles measured at a concentration of 1.30×10^{-5} M MB dye solution, (**b**) cyclic voltammetry measurement in 2.30×10^{-5} M MB dye solution at different scan rates, (**c**) current density for (ECSA) along with linear fitting of different anodic and cathodic measurements, and (**d**) EIS measurement at a concentration of 2.30×10^{-5} M MB dye solution under the illumination of ultraviolet light at a sweeping 100 kHz to 0.1 Hz, an amplitude of mV, and zero-bias potential in open circuit.

3. Experimental Section

3.1. Chemical and Reagents

Chemicals of high analytical grade were obtained from Merck and Sigma Aldrich, Karachi, Sindh, Pakistan. Among these are ascorbic acid (C6H8O6, Mm 176.12 g/mol), sodium borohydride (NaBH4, Mm 37.83 g/mol), sodium hydroxide, hydrochloric acid, and methylene blue (C16H18ClN3S, Mm 319.85 g/mol). Deionized water was used throughout the study to prepare desired solutions.

3.2. Synthesis of Carbon Material from C. papaya Fruit

A typical method of preparing carbon material was developed and described in Scheme 1. Initially, low-quality *C. papaya* fruit was obtained from the local market of Jamshoro, Sindh, Pakistan. Afterwards, the fruit mass was chopped into small pieces and then juiced using a juicer machine. A muffle furnace was then used to heat 50 mL of *C. papaya* juice at 220 °C for 2 h at a ramp rate of 15 °C per minute. A glass beaker containing DI water was filled with the resultant carbonized material (2 g). The solution was sonicated for 50 min and then centrifuged for 30 min at 5000 rotations per minute in order to remove the larger carbon particles. We were finally able to obtain a dark brown carbon material (0.4 g) for further analysis.

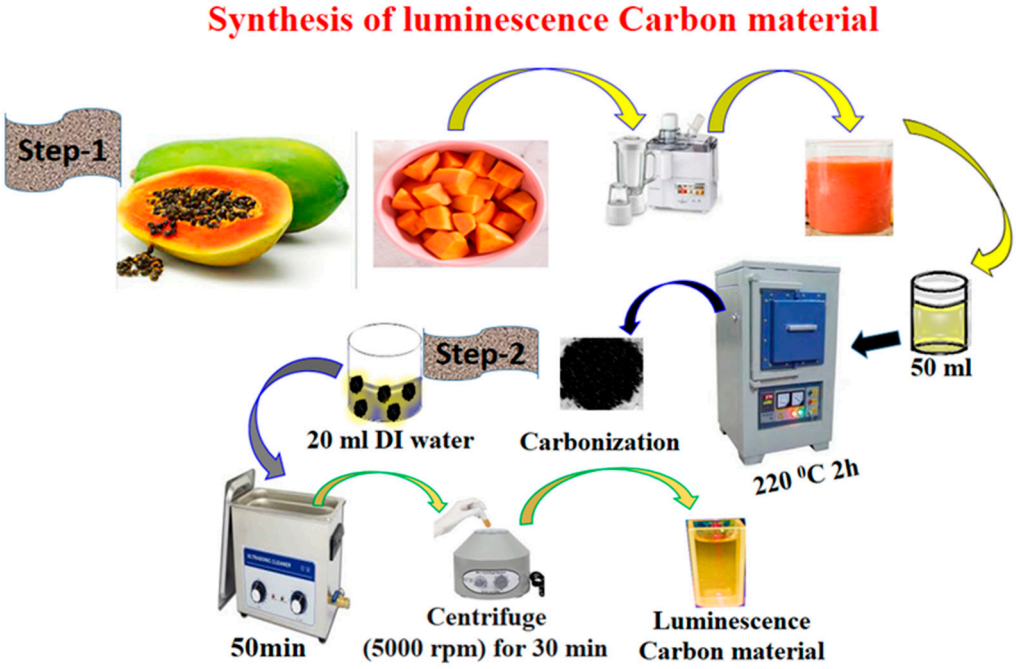

Scheme 1. Schematic illustration showing the synthesis of carbon material from *Carica papaya* juice.

3.3. Characterizations of Prepared Carbon Material

The crystalline structure was investigated using X-ray diffraction (XRD) *(Cu Kα radiation with λ of 0.15406 nm at scanning at range of 10–80°, Bruker D8 advance)*. The morphology of carbon material prepared from *C. papaya* fruit was investigated using scanning electron microscopy (*SEM, Hitachi Regulus 8100*, Tokyo, Japan) at a voltage of 20 KV using SEM. FT-IR spectrometer (*Tensor 27, Bruker Optics, Ettlingen, Germany*) was used to characterize the functional groups. Finally, UV-visible spectroscopy (*Lamda 365, PerkinElmer, Waltham, MA, USA*) was used to measure the absorbance of model dye methylene blue in the 200–800 wavelength range.

3.4. Photocatalytic Application of Carbon Material Derived from C. papaya

An evaluation of the photodegradation performance of methylene blue (MB) dye was conducted under UV illumination. As part of the photocatalytic study, an aqueous solution of (2.3×10^{-5} M) and (1.15×10^{-5} M) of MB was prepared, and different doses of 5 mg, 10 mg, and 15 mg of the dye solution 2.3×10^{-5} M MB were transferred into separate glass beakers containing 50 mL of 2.3×10^{-5} M MB solution, which was then exposed to UV radiation. A UV light box containing six light-emitting diodes (LEDs) of 365 nm and 10 W power was used. Additionally, 2 mL of each irradiated MB solution was placed in a quartz cell and the change in absorbance for different time intervals was measured using a UV-vis

spectrophotometer. Calculation of dye removal percentage (% D) from prepared carbon material was conducted using Equation (1).

$$\% \, D = \frac{A_0 - A_t}{A_0} \times 100\% \quad (1)$$

where A_0 represents absorbance of the initial concentration of MB dye (before illumination) and A_t indicates the change in concentration of MB dye (after illumination) at time 't'. However, the degradation rate constant of MB dye was calculated by using the Langmuir–Hinshelwood kinetic model. The photocatalytic degradation process of methylene blue was stated by the pseudo-first-order kinetic Equation (2).

$$\ln(C_0/C_t) = kt \quad (2)$$

Herein, k symbolizes the apparent reaction rate constant (min^{-1}), C_0 expresses the initial dye concentration (MB), and C_t illustrates the dye concentration at illumination time.

We used a 2.3×10^{-5} M MB dye solution to determine the effect of pH on the degradation of prepared carbon materials, and we then altered the pH using 0.2 M HCl and NaOH aqueous solutions. Additionally, scavenger tests were performed in order to determine the type of radical responsible for the breakdown of MB under UV radiation. With a dye solution containing 2.3×10^{-5} M dye, the degradation performance of the newly prepared carbon material was evaluated. The pH of the solution was adjusted with 0.2 M HCl and NaOH solutions. In addition, scavenger studies were conducted in order to investigate the nature of the radicals involved in the degradation of MB in the presence of UV light. Hence, ascorbic acid ($C_6H_8O_6$), ethylenediamine tetracetate acid disodium (EDTA-Na_2), and sodium monohydrate ($NaBH_4$) were some of the scavengers we employed in the MB solution. We used a concentration of 10 mM for each scavenger, and we added 15 mg of carbon material to 60 µL of MB solution. Measurements of scavengers were conducted under UV illumination. To examine the role of active surface area and charge transfer, cyclic voltammetry and electrochemical impedance spectroscopy were employed. A non-Faradic region of CV curves at different scan rates in 2.3×10^{-5} M was used first to determine the electrochemical active surface area. During the electrochemical testing, three electrode configurations were used, including a silver–silver reference electrode holding 3M KCl mixture, a platinum wire counter electrode, and a glassy carbon working electrode. Before the electrochemical measurement, the glassy carbon electrode was polished with alumina paste and silicon paper and rinsed several times with DI water. In the following step, 5 mg of carbon material was dispersed in 3 mL of deionized water and 100 mL of 5% Nafion solution to create a photocatalyst slurry. A drop-casting technique was then employed to drop 10 µL (0.2 milligrams) of photocatalyst ink onto a glassy carbon electrode. We allowed the modified electrode to dry in the open air for a period of time. An electrode composed of of glassy carbon had a surface area of approximately three millimeters. For the EIS investigations, the sweeping frequency was 100 kHz to 0.01 Hz, with a biasing potential of zero and an amplitude of 10 mV.

An electrochemical workstation was used to carry out the EIS in a 2.3×10^{-5} M MB dye under UV irradiation. An estimate of the current density was obtained by dividing the measured current by the area of a glassy carbon electrode. With the assistance of Z-view software, EIS data were simulated using a well-fitted equivalent circuit in order to calculate the charge transfer rate of carbon material during the breakdown of MB. In order to determine the size distribution of carbon material, 3 mg of carbon material was dispersed in 10 mL of deionized water (ZS) using the Malvern Zetasizer Nano.

4. Conclusions

As a conclusion, we have utilized the pyrolytic method to synthesize a carbon-based photocatalyst from *Carica papaya* juice for the first time due to its low cost, simplicity, ease of scaling, eco-friendliness, and environmental friendliness. It has been extensively studied in

terms of the shape, crystalline properties, particle size distribution, and optical properties of this newly prepared carbon material. For the first time, the newly prepared carbon material from *Carica papaya* juice was employed for the photodegradation of MB in aqueous solution. It has demonstrated superior catalytic properties compared to previously reported carbon materials. The different parameters that influence the performance evolution of the presented photocatalyst have been investigated, including the initial dye concentration, catalyst dose, pH of the dye solution, cyclic stability, and identification of the dominant oxidizing radical. In consequence, a degradation efficiency of approximately 99.67% was obtained, and a first-order kinetics model was used to describe the degradation process. It was found that the degradation rate was highly dependent on the initial dye concentration, the pH of the dye solution, and the catalyst dose. The use of *Carica papaya* juice as a green and natural raw material for the synthesis of efficient carbon-based photocatalytic material offers a new roadmap for the development of new photocatalytic materials for environmental and solar-driven hydrogen production applications.

Author Contributions: M.A.B., did the material synthesis and partial photocatalytic measurements; E.D., did validate the results; A.T., did XRD and FTIR studies; K.F.A., partially supervised work; S.S.M., did DLS analysis and proposed the scavenger studies; A.N., did proofread and analyzed the photocatalytic results; Z.A.S., did SEM analysis; U.A., did EIS and ECSA analysis; Z.H.I., did main supervision and wrote the first draft of manuscript. All authors have read and agreed to the published version of the manuscript.

Funding: This research received no external funding.

Institutional Review Board Statement: Not applicable.

Informed Consent Statement: Not application.

Data Availability Statement: All research data is included in this article.

Acknowledgments: The authors gratefully acknowledge the Higher Education Commission Pakistan for partial support under project NRPU/8350. We also extend our sincere appreciation to the Researchers Supporting Project Number (RSP2023R79) at King Saud University, Riyadh, Saudi Arabia. Authors also acknowledge the partial funding from Ajman University, Grant ID: DRGS ref. 2022-IRG-HBS-5.

Conflicts of Interest: Authors declare no competing interest in the presented research work.

References

1. Arul, V.; Sethuraman, M.G. Hydrothermally green synthesized nitrogen-doped carbon dots from Phyllanthus emblica and their catalytic ability in the detoxification of textile effluents. *ACS Omega* **2019**, *2*, 3449–3457. [CrossRef] [PubMed]
2. Wang, S.; Sun, H.; Ang, H.M.; Tadé, M.O. Adsorptive remediation of environmental pollutants using novel graphene-based nanomaterials. Chem. *Eng. J.* **2013**, *226*, 336–347.
3. Saleh, T.A. The Role of Carbon Nanotubes in Enhancement of Photocatalysis. In *Syntheses and Applications of Carbon Nanotubes and Their Composite*; SAGE Publishing: New York, NY, USA, 2013; pp. 479–493.
4. Zhai, W.; Li, G.; Yu, P.; Yang, L.; Mao, L. Silver phosphate/carbon nanotube-stabilized Pickering emulsion for highly efficient photocatalysis. *J. Phys. Chem. C* **2013**, *117*, 15183–15191. [CrossRef]
5. Jiang, G.; Lin, Z.; Zhu, L.; Ding, Y.; Tang, H. Preparation and photoelectrocatalytic properties of titania/carbon nanotube composite films. *Carbon* **2010**, *48*, 3369–3375. [CrossRef]
6. Jiao, X.L.; Abbas, T.; Ahmad, M.; Ahmed, E.; Hong, Z.L.; Khalid, N.R. Enhancement in visible light-responsive photocatalytic activity by embedding Cu-doped ZnO nanoparticles on multi-walled carbon nanotubes. *Appl. Surf. Sci.* **2013**, *285*, 702–712.
7. Zhang, J.; Yao, Y.; Chen, H.; Wu, G.; Qin, J.; Lian, C.; Wang, S. Iron encapsulated in boron and nitrogen codoped carbon nanotubes as synergistic catalysts for Fenton-like reaction. *Water Res.* **2016**, *101*, 281–291.
8. Khatibi, E.S.; Haghighi, M.; Mahboob, S. Efficient surface design of reduced graphene oxide, carbon nanotube and carbon active with cupper nanocrystals for enhanced simulated-solar-light photocatalytic degradation of acid orange in water. *Appl. Surf. Sci.* **2019**, *465*, 937–949. [CrossRef]
9. Yang, S.; Wang, L.; Zhang, X.; Yang, W.; Song, G. Enhanced adsorption of Congo red dye by functionalized carbon nanotube/mixed metal oxides nanocomposites derived from layered double hydroxide precursor. *Chem. Eng. J.* **2015**, *275*, 315–321. [CrossRef]
10. Mallakpour, S.; Khadem, E. Carbon nanotube–metal oxide nanocomposites: Fabrication, properties and applications. *Chem. Eng. J.* **2016**, *302*, 344–367. [CrossRef]

11. Wang, L.; Zhou, H.S. Green synthesis of luminescent nitrogen-doped carbon dots from milk and its imaging application. *Anal. Chem.* **2014**, *18*, 8902–8905. [CrossRef]
12. Lu, W.; Qin, X.; Liu, S.; Chang, G.; Zhang, Y.; Luo, Y.; Asiri, A.M.; Al-Youbi, A.O.; Sun, X. Economical, green synthesis of fluorescent carbon nanoparticles and their use as probes for sensitive and selective detection of mercury (II) ions. *Anal. Chem.* **2012**, *12*, 5351–5357. [CrossRef] [PubMed]
13. Song, Y.; Yan, X.; Li, Z.; Qu, L.; Zhu, C.; Ye, R.; Li, S.; Du, D.; Lin, Y. Highly photoluminescent carbon dots derived from linseed and their applications in cellular imaging and sensing. *J. Mater. Chem. B* **2018**, *19*, 3181–3187. [CrossRef] [PubMed]
14. Liang, Z.; Zeng, L.; Cao, X.; Wang, Q.; Wang, X.; Sun, R. Sustainable carbon quantum dots from forestry and agricultural biomass with amplified photoluminescence by simple NH 4 OH passivation. *J. Mater. Chem. C* **2014**, *45*, 9760–9766. [CrossRef]
15. Wu, Z.L.; Zhang, P.; Gao, M.X.; Liu, C.F.; Wang, W.; Leng, F.; Huang, C.Z. One-pot hydrothermal synthesis of highly luminescent nitrogen-doped amphoteric carbon dots for bioimaging from Bombyx mori silk–natural proteins. *J. Mater. Chem. B* **2013**, *22*, 2868–2873. [CrossRef] [PubMed]
16. KyungáJung, Y. Sweet nanodot for biomedical imaging: Carbon dot derived from xylitol. *Rsc Adv.* **2014**, *44*, 23210–23213.
17. Atchudan, R.; Edison, T.N.J.I.; Sethuraman, M.G.; Lee, Y.R. Efficient synthesis of highly fluorescent nitrogen-doped carbon dots for cell imaging using unripe fruit extract of Prunus mume. *Appl. Surf. Sci.* **2016**, *384*, 432–441. [CrossRef]
18. Jawad, A.H.; Ngoh, Y.S.; Radzun, K.A. Utilization of watermelon (*Citrullus lanatus*) rinds as a natural low-cost biosorbent for adsorption of methylene blue: Kinetic, equilibrium and thermodynamic studies. *J. Taibah Univ. Sci.* **2018**, *4*, 371–381. [CrossRef]
19. Ibrahim, A.; Yusof, L.; Beddu, N.S.; Galasin, N.; Lee, P.Y.; Lee, R.N.S.; Zahrim, A.Y. June. Adsorption study of Ammonia Nitrogen by watermelon rind. In *IOP Conference Series: Earth and Environmental Science*; IOP Publishing: Bristol, UK, 2016; Volume 36, p. 012020.
20. Treml, J.; Šmejkal, K. Flavonoids as potent scavengers of hydroxyl radicals. *Compr. Rev. Food Sci. Food Saf.* **2016**, *4*, 720–738. [CrossRef]
21. Yang, Y.; Cui, J.; Zheng, M.; Hu, C.; Tan, S.; Xiao, Y.; Yang, Q.; Liu, Y. One-step synthesis of amino-functionalized fluorescent carbon nanoparticles by hydrothermal carbonization of chitosan. *Chem. Commun.* **2012**, *48*, 380–382. [CrossRef]
22. Tetsuka, H.; Asahi, R.; Nagoya, A.; Okamoto, K.; Tajima, I.; Ohta, R.; Okamoto, A. Optically tunable amino-functionalized graphene quantum dots. *Adv. Mater.* **2012**, *24*, 5333–5338. [CrossRef]
23. Jin, S.H.; Kim, D.H.; Jun, G.H.; Hong, S.H.; Jeon, S. Tuning the photoluminescence of graphene quantum dots through the charge transfer effect of functional groups. *ACS Nano* **2013**, *7*, 1239–1245. [CrossRef]
24. Sugiarti, S.; Darmawan, N. Synthesis of fluorescence carbon nanoparticles from ascorbic acid. *Indones. J. Chem.* **2015**, *15*, 141–145. [CrossRef]
25. Zhang, Z.; Sun, W.; Wu, P. Highly photoluminescent carbon dots derived from egg white: Facile and green synthesis, photoluminescence properties, and multiple applications. *ACS Sustain. Chem. Eng.* **2015**, *3*, 1412–1418. [CrossRef]
26. Eda, G.; Lin, Y.Y.; Mattevi, C.; Yamaguchi, H.; Chen, H.A.; Chen, I.S.; Chen, C.W.; Chhowalla, M. Blue photoluminescence from chemically derived graphene oxide. *Adv. Mater.* **2010**, *22*, 505–509. [CrossRef]
27. Pan, D.Y.; Zhang, J.C.; Li, Z.; Wu, M.H. Hydrothermal Route for Cutting Graphene Sheets into Blue-Luminescent Graphene Quantum Dots. *Adv. Mater.* **2010**, *22*, 734–738. [CrossRef] [PubMed]
28. Zheng, M.; Xie, Z.G.; Qu, D.; Li, D.; Du, P.; Jing, X.B.; Sun, Z.C. On-Off-On Fluorescent Carbon Dot Nanosensor for Recognition of Chromium(VI) and Ascorbic Acid Based on the Inner Filter Effect. *ACS Appl. Mater. Interfaces* **2013**, *5*, 13242–13247. [CrossRef]
29. Wang, W.J.; Hai, X.; Mao, Q.X.; Chen, M.L.; Wang, J.H. Polyhedral oligomeric silsesquioxane functionalized carbon dots for cell imaging. *ACS Appl. Mater. Interfaces* **2015**, *7*, 16609–16616. [CrossRef]
30. Wang, T.; Wang, A.; Wang, R.; Liu, Z.; Sun, Y.; Shan, G.; Liu, Y. Carbon dots with molecular fluorescence and their application as a "turn-off" fluorescent probe for ferricyanide detection. *Sci. Rep.* **2019**, *9*, 1–9. [CrossRef]
31. Zandrini, T.; Shan, O.; Parodi, V.; Cerullo, G.; Raimondi, M.T.; Osellame, R. Multi-foci laser microfabrication of 3D polymeric scaffolds for stem cell expansion in regenerative medicine. *Sci. Rep.* **2019**, *9*, 11761. [CrossRef]
32. Guo, J.; Dong, F.; Zhong, S.; Zhu, B.; Huang, W.; Zhang, S. TiO_2–hydroxyapatite composite as a new support of highly active and sintering-resistant gold nanocatalysts for catalytic oxidation of CO and photocatalytic degradation of methylene blue. *Catal. Lett.* **2018**, *148*, 359–373. [CrossRef]
33. Singh Vig, A.; Gupta, A.; Pandey, O.P. Efficient photodegradation of methylene blue (MB) under solar radiation by ZrC nanoparticles. *Adv. Powder Technol.* **2018**, *29*, 2231–2242. [CrossRef]
34. Mallakpour, S.; Hatami, M. LDH-VB9-TiO_2 and LDH-VB9-TiO_2/crosslinked PVA nanocomposite prepared via facile and green technique and their photo-degradation application for methylene blue dye under ultraviolet illumination. *Appl. Clay Sci.* **2018**, *163*, 235–248. [CrossRef]
35. Pouretedal, H.R.; Kadkhodaie, A. Synthetic CeO_2 nanoparticle catalysis of methylene blue photodegradation: Kinetics and mechanism. *Chin. J. Catal.* **2010**, *31*, 1328–1334. [CrossRef]
36. Jing, H.P.; Wang, C.C.; Zhang, Y.W.; Wang, P.; Li, R. Photocatalytic degradation of methylene blue in ZIF-8. *RSC Adv.* **2014**, *4*, 54454–54462. [CrossRef]
37. Akpan, U.G.; Hameed, B.H. Parameters affecting the photocatalytic degradation of dyes using TiO_2-based photocatalysts: A review. *J. Hazard. Mater.* **2009**, *170*, 520–529. [CrossRef]

38. Wen, L.L.F.; Wang, J.; Feng, L.; Lv, C.G.; Wang, C.G.; Li, D.F. Structures, photoluminescence, and photocatalytic properties of six new metal-organic frameworks based on aromatic polycarboxylate acids and rigid imidazole-based synthons. *Cryst. Growth Des.* **2009**, *9*, 3581–3589. [CrossRef]
39. Sunil, G.S.; Vilas, K.M.; Sandip, P.P.; Gunvant, H.S. Effect of doping parameters on photocatalytic degradation of methylene blue using Ag doped ZnO nanocatalyst. *SN Appl. Sci.* **2020**, *2*, 820.
40. Chong, M.N.; Jin, B.; Chow, C.W.K.; Saint, C. Recent developments in photocatalytic water treatment technology: A review. *Water Res.* **2010**, *44*, 2997–3027. [CrossRef]
41. Mondol, B.; Sarker, A.; Shareque, A.M.; Dey, S.C.; Islam, M.T.; Das, A.K.; Shamsuddin, S.M.; Molla, M.A.I.; Sarker, M. Preparation of Activated Carbon/TiO_2 Nanohybrids for Photodegradation of Reactive Red-35 Dye Using Sunlight. *Photochem* **2021**, *1*, 54–66. [CrossRef]
42. Molla, M.A.I.; Tateishi, I.; Furukawa, M.; Katsumata, H.; Suzuki, T.; Kaneco, S. Evaluation of Reaction Mechanism for Photocatalytic Degradation of Dye with Self-Sensitized TiO_2 under Visible Light Irradiation. *Open J. Inorg. Non-Met. Mater.* **2017**, *7*, 1–7
43. Laghari, A.J.; Aftab, U.; Tahira, A.; Shah, A.A.; Gradone, A.; Solangi, M.Y.; Samo, A.H.; Kumar, M.; Abro, M.I.; Akhtar, M.W.; et al. MgO as promoter for electrocatalytic activities of Co_3O_4–MgO composite via abundant oxygen vacancies and Co^{2+} ions towards oxygen evolution reaction. *Int. J. Hydrog. Energy* **2022**, *48*, 12672–12682. [CrossRef]
44. Hartanto, D.; Yuhaneka, G.; Utomo, W.P.; Rozafia, A.I.; Kusumawati, Y.; Dahani, W.; Iryani, A. Unveiling the charge transfer behavior within ZSM-5 and carbon nitride composites for enhanced photocatalytic degradation of methylene blue. *RSC Adv.* **2022**, *12*, 5665–5676. [CrossRef] [PubMed]